

# Properties of the Neutrino Mixing Matrix

S. H. Chiu\*

*Physics Group, CGE, Chang Gung University, Kwei-Shan 333, Taiwan*

T. K. Kuo†

*Department of Physics, Purdue University, West Lafayette, IN 47907, USA*

## Abstract

For neutrino mixing we propose to use the parameter set  $X_i (= |V_{ei}|^2)$  and  $\Omega_i (= \epsilon_{ijk}|V_{\mu j}|^2|V_{\tau k}|^2)$ , with two constraints. These parameters are directly measurable since the neutrino oscillation probabilities are quadratic functions of them. Physically, the set  $\Omega_i$  signifies a quantitative measure of  $\mu - \tau$  asymmetry. Available neutrino data indicate that all the  $\Omega_i$ 's are small ( $\lesssim O(10^{-1})$ ), but with large uncertainties. The behavior of  $\Omega_i$  as functions of the induced neutrino mass in matter are found to be simple, which should facilitate the analyses of long baseline experiments.

arXiv:1210.7061v2 [hep-ph] 6 Nov 2012

---

\* schiu@mail.cgu.edu.tw

† tkkuo@purdue.edu

## I. INTRODUCTION

The recent results from the  $\bar{\nu}$  disappearance experiments [1, 2] have made important contributions toward pinning down the elements of the neutrino mixing (PMNS) matrix, which we will denote as  $V_\nu$ , with elements  $V_{\alpha i}$ ,  $\alpha = (e, \mu, \tau)$ ,  $i = (1, 2, 3)$ . Of the four physical parameters in  $V_\nu$ , three have now been measured, albeit with different degrees of accuracy. Furthermore, some information on the fourth can already be gleaned from the known data set obtained by the various extant experiments, as was done in global analyses thereof (see, *e.g.*, [3, 4]). It seems timely to study the available results in detail, with the intent to extract some general properties of  $V_\nu$  which may be used to suggest directions for further investigation.

In this paper we will concentrate on two aspects of  $V_\nu$ . First, it is interesting to assess the impact of the known results on the possible symmetry properties of  $V_\nu$ . Next, we address the behaviour of  $V_\nu$  as a function of the parameter  $A = 2\sqrt{2}G_F n_e E$ , the induced neutrino mass in matter. This is especially relevant to the long baseline experiments (LBL) (for an incomplete list, see, *e.g.*, Ref.[5, 6] and the references therein), which are generally regarded as the “future” of neutrino physics explorations.

The analyses of these issues are facilitated by a judicious choice of parameters for  $V_\nu$ . To begin, in this study we will use the rephasing invariant parametrization introduced earlier. It consists of six parameters  $(x_i, y_j)$ , which satisfy two constraints. Prior to the recent measurement on  $\bar{\nu}_e \rightarrow \bar{\nu}_e$ , which results in a “large”  $|V_{e3}|$ , it seems probable that  $V_\nu$  is  $\mu - \tau$  symmetric [7, 8],  $|V_{\mu i}| = |V_{\tau i}|$ . These conditions, when expressed in the variables  $\Omega_i = x_i + y_i$ , are just  $\Omega_i = 0$ . Now that  $|V_{e3}|$  is non-vanishing, exact  $\mu - \tau$  symmetry becomes less likely. The question remains: “Is there an approximate  $\mu - \tau$  symmetry, and how good is it?”. It seems natural, then, to interpret  $\Omega_i$  as the  $\mu - \tau$  symmetry-breaking parameters. As we shall see, they satisfy a constraint and thus there are only two independent parameters in the set  $\Omega_i$ . Also, taken together, the known neutrino data actually constrain all the  $\Omega_i$ ’s so that none of which deviate much from zero. The other physical parameters we choose are  $X_i = x_i - y_i = |V_{ei}|^2$ . As we shall see, the set  $(X_i, \Omega_i)$  is convenient for studying  $V_\nu$ , in vacuum as well as in matter..

For neutrino propagation in matter, it turns out that  $X_i$ , together with  $\Delta_{ij} = m_i^2 - m_j^2$ , satisfy a set of differential equations with respect to  $A$ , the induced mass. Experimentally, the  $X_i$ ’s and  $\Delta_{ij}$ ’s are all very well measured in vacuum ( $A = 0$ ). This means that  $X_i$  and  $\Delta_{ij}$  are well determined, for all values of  $A$ . Separately,  $\Omega_i$  satisfy a set of differential equations containing  $X_i$  and  $\Delta_{ij}$ . They can be integrated to obtain  $\Omega_i(A)$ , with the known solution of  $(X_i, \Delta_{ij})$  as inputs. Here, however, the initial values are poorly determined since there is only one direct measurement (from atmospheric neutrinos) on  $\Omega_1 - \Omega_2$ , with large errors. Nevertheless, it will be seen that the  $\Omega_i(A)$ ’s are largely constrained.

To go forward, our analysis suggests that the most urgent task would be another independent measurement on  $\Omega_i$ . It will clarify the nature of  $V_\nu$  to a large extent. At the same time, the close correlation between vacuum parameters and those in matter also means that LBL experiments with variable  $A$  can be extremely useful in the study of  $V_\nu$ .

## II. REPHASING INVARIANT PARAMETRIZATION

As was shown before [9–12], one can construct rephasing invariant combinations out of elements of a unitary, unimodular ( $\det V = +1$ , so that  $V^* =$  matrix of cofactors of  $V$ ),

mixing matrix,

$$\Gamma_{ijk} = V_{1i}V_{2j}V_{3k} = R_{ijk} - iJ, \quad (1)$$

where their common imaginary part can be identified with the Jarlskog invariant  $J$  [16]. Their real parts are defined as

$$(R_{123}, R_{231}, R_{312}; R_{132}, R_{213}, R_{321}) = (x_1, x_2, x_3; y_1, y_2, y_3). \quad (2)$$

These variables are bounded by  $\pm 1$ :  $-1 \leq (x_i, y_j) \leq +1$ , with  $y_j \leq x_i$  for any  $(i, j)$ . They satisfy two constraints

$$\det V = (x_1 + x_2 + x_3) - (y_1 + y_2 + y_3) = 1, \quad (3)$$

$$(x_1x_2 + x_2x_3 + x_3x_1) - (y_1y_2 + y_2y_3 + y_3y_1) = 0. \quad (4)$$

In addition, it is found that

$$J^2 = x_1x_2x_3 - y_1y_2y_3. \quad (5)$$

Thus, the physical parameters contained in  $V$  can be specified by the set  $(x, y)$  plus a sign, corresponding to  $J = \pm\sqrt{J^2}$ .

For applications to neutrino physics, it is traditional to label the matrix elements as  $V_{\alpha i}$ ,  $\alpha = (e, \mu, \tau)$ ,  $i = (1, 2, 3)$ . The relations between  $(x, y)$  and  $|V_{\alpha i}|^2$  are given by

$$W = [|V_{\alpha i}|^2] = \begin{pmatrix} x_1 - y_1 & x_2 - y_2 & x_3 - y_3 \\ x_3 - y_2 & x_1 - y_3 & x_2 - y_1 \\ x_2 - y_3 & x_3 - y_1 & x_1 - y_2 \end{pmatrix}. \quad (6)$$

One can readily obtain the parameters  $(x, y)$  from  $W$  by computing its cofactors, which form the matrix  $w$  with  $w^T W = (\det W)I$ , and is given by

$$w = \begin{pmatrix} x_1 + y_1 & x_2 + y_2 & x_3 + y_3 \\ x_3 + y_2 & x_1 + y_3 & x_2 + y_1 \\ x_2 + y_3 & x_3 + y_1 & x_1 + y_2 \end{pmatrix}. \quad (7)$$

Note that the elements of  $w$  are bounded,  $-1 \leq w_{\alpha i} \leq +1$ , and

$$\sum_i w_{\alpha i} = \sum_{\alpha} w_{\alpha i} = \det W, \quad (8)$$

$$\det W = \sum x_i^2 - \sum y_j^2 = \sum x_i + \sum y_j, \quad (9)$$

where the constraint equations Eq. (3) and Eq. (4) have been used.

The constraints Eqs. (3) and (4) can be easily derived by using the identity  $\Gamma_{123}\Gamma_{231}\Gamma_{312} = \Gamma_{132}\Gamma_{213}\Gamma_{321}$ . One can obtain other useful relations when we consider product of the form  $\Gamma_{ijk}\Gamma_{lmn}$ . Thus, the well-known rephasing invariant expression  $\Pi_{ij}^{\alpha\beta} = V_{\alpha i}V_{\beta j}V_{\alpha j}^*V_{\beta i}^*$  consists of four such terms. For instance,

$$\begin{aligned} \Pi_{23}^{e\mu} &= (y_1 - iJ)(y_2 - iJ) - (x_2 - iJ)(x_3 - iJ) \\ &\quad - (x_1 - iJ)(x_2 - iJ) + (x_2 - iJ)(y_3 - iJ). \end{aligned} \quad (10)$$

The combination  $\Pi_{ij}^{\alpha\beta}$  has the additional property that it is rephasing invariant even if  $\det V = e^{i\theta} \neq 1$ . Another useful formula (with  $\det V = +1$ ) is

$$\begin{aligned}\Pi_{ij}^{\alpha\beta} &= |V_{\alpha i}|^2 |V_{\beta j}|^2 - \sum_{\gamma k} \epsilon_{\alpha\beta\gamma} \epsilon_{ijk} V_{\alpha i} V_{\beta j} V_{\gamma k} \\ &= |V_{\alpha j}|^2 |V_{\beta i}|^2 + \sum_{\gamma k} \epsilon_{\alpha\beta\gamma} \epsilon_{ijk} V_{\alpha j}^* V_{\beta i}^* V_{\gamma k}^*,\end{aligned}\quad (11)$$

where the second term in either expression is one of the  $\Gamma$ 's ( $\Gamma^*$ 's) defined in Eq. (1).

We now turn to combinations of the form  $(y_l - iJ)(y_m - iJ) - (x_i - iJ)(x_j - iJ)$ . As an explicit example, consider  $(y_1 - iJ)(y_2 - iJ) - (x_1 - iJ)(x_2 - iJ) = (y_1 y_2 - x_1 x_2) + iJ(x_1 + x_2 - y_1 - y_2)$ , or

$$V_{e1} V_{e2} V_{e3}^* V_{\mu 3} V_{\tau 3} = (y_1 y_2 - x_1 x_2) + iJ(1 - |V_{e3}|^2). \quad (12)$$

In general, for  $\alpha \neq \beta \neq \gamma$ ,  $i \neq j \neq k$ ,

$$V_{\alpha j} V_{\alpha k} V_{\alpha i}^* V_{\beta i} V_{\gamma i} = (y_m y_n - x_b x_c) + iJ(1 - |V_{\alpha i}|^2). \quad (13)$$

Here, if  $|V_{\alpha i}|^2 = x_a - y_l$ , then  $b \neq c \neq a$ ,  $m \neq n \neq l$ . Thus, if we take the matrix elements in the  $\alpha$ -th row and the  $i$ -th column, complex conjugate the vertex ( $V_{\alpha i}^*$ ), then the product is rephasing invariant and has a well-defined imaginary part. In fact, Eq. (13) provides another way to compute  $J$ . For instance, in the standard parametrization [13], if we take  $\alpha = e$  and  $i = 3$ , we quickly recover the usual expression for  $J$ . The real part of Eq. (13) is also useful. It enables us to compute other physical variables and, if  $|V_{\alpha i}| \ll 1$ , set stringent bounds on them. We will discuss these applications in sec. IV and V.

### III. CHOICE OF VARIABLES

Over the past couple of decades, a wealth of information has been gathered by neutrino oscillation experiments. It would be useful to analyze the available data systematically so as to gain an overview of the neutrino mixing matrix. To this end it is important to choose a set of parameters which can bring out clearly the salient features of  $V_\nu$ . In this paper we propose to use certain combinations of the variables  $(x, y)$  which, as we shall see, can highlight the symmetry properties of  $V_\nu$ . In addition, they have simple behaviors when used in the study of neutrino propagation in matter.

Specifically, we choose the parameters,

$$X_i = x_i - y_i = |V_{ei}|^2 = W_{ei}, \quad (14)$$

$$\Omega_i = x_i + y_i = \epsilon_{ijk} W_{\mu j} W_{\tau k} = w_{ei}, \quad (15)$$

where  $i = (1, 2, 3)$ . Note that  $-1 \leq \Omega_i \leq 1$ , and

$$W_{\mu i} - W_{\tau i} = -\frac{1}{2} \epsilon_{ijk} (\Omega_j - \Omega_k), \quad (16)$$

$$4J^2 = X_1 X_2 X_3 + X_1 \Omega_2 \Omega_3 + X_2 \Omega_1 \Omega_3 + X_3 \Omega_1 \Omega_2. \quad (17)$$

These variables are considered to be functions of  $A = 2\sqrt{2}G_F n_e E$ , the induced neutrino mass, which will be used when we discuss neutrino propagation in matter. For the specific case of vacuum values,  $A = 0$ , we will use the notation  $X_i^0$  and  $\Omega_i^0$ .

The variables  $X_i$  and  $\Omega_i$  are not independent. Obviously,

$$\sum X_i = 1. \quad (18)$$

The set  $\Omega_i$  also satisfies a simple constraint. From

$$W_{ei}w_{ei} = \det W, \quad (19)$$

and, using Eqs. (3) and (4),

$$\det W = \sum x_i^2 - \sum y_j^2 = \sum x_i + \sum y_j = \sum \Omega_i, \quad (20)$$

we find

$$\sum \Omega_i(1 - X_i) = 0 \quad (21)$$

The two constraints Eqs. (18) and (21) are equivalent to Eqs. (3) and (4), but Eq. (21) is easier to implement since it is linear in  $\Omega_i$ . Note also that if all the  $\Omega_i$ 's are equal, as happens when  $W_{\mu i} = W_{\tau i}$ , then  $\Omega_i = 0$ .

Thus, the rephasing invariant parametrization of  $V_\nu$  consists of the set  $(X_i, \Omega_i)$ , subject to two constraints, Eqs. (18) and (21). Together with the mass differences,  $\Delta_{ij} = D_i - D_j$ ,  $D_i = m_i^2$ , they form a complete set of parameters for the neutrino oscillation phenomenology.

Before the recent measurements of  $|V_{e3}|^2$ , the possibility of a vanishing  $|V_{e3}|^2$  and the equality  $W_{\mu 3} = W_{\tau 3}$  led to the hypothesis of  $\mu - \tau$  exchange symmetry for neutrino mixing,  $W_{\mu i} = W_{\tau i}$ . With the confirmed small, but non-vanishing,  $|V_{e3}|^2$ ,  $\mu - \tau$  symmetry becomes less likely (although not excluded). Nevertheless, it is interesting to analyze the property of  $V_\nu$  under the  $\mu - \tau$  exchange operation. To this end, let us introduce a  $\mu - \tau$  parity operator,  $P_{\mu\tau}$ , such that

$$P_{\mu\tau} : W_{\mu i} \leftrightarrow W_{\tau i}. \quad (22)$$

From  $X_i = 1 - (W_{\mu i} + W_{\tau i})$  and Eq. (15), we find

$$P_{\mu\tau} : X_i \leftrightarrow X_i, \quad (23)$$

$$P_{\mu\tau} : \Omega_i \leftrightarrow -\Omega_i, \quad (24)$$

In addition, since a  $\mu - \tau$  exchange does not affect the eigenvalues of the neutrino mass matrix, we also have

$$P_{\mu\tau} : \Delta_{ij} \leftrightarrow \Delta_{ij}. \quad (25)$$

These results are independent of  $A$ , since the matter effect only contributes to the  $e - e$  element of the effective neutrino Hamiltonian. Finally, from Eq. (17), we see that  $J^2$  is also invariant under  $P_{\mu\tau}$ ,  $J^2 \leftrightarrow J^2$ .

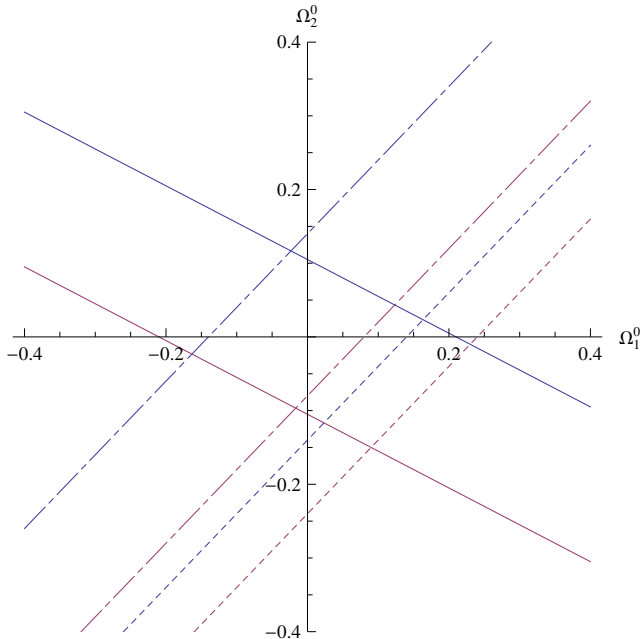
Thus, the neutrino parameters can be classified as 1) even under  $P_{\mu\tau} : X_i, \Delta_{ij}, J^2$ ; 2) odd under  $P_{\mu\tau} : \Omega_i$ . The quantities  $\Omega_i$  serve as symmetry-breaking parameters – they provide a measure of how good/bad the  $\mu - \tau$  exchange symmetry is.

We summarize our results in the matrix:

$$W_\nu = \begin{pmatrix} X_1 & X_2 & X_3 \\ \frac{1}{2}[(1 - X_1) + (\Omega_3 - \Omega_2)] & \frac{1}{2}[(1 - X_2) + (\Omega_1 - \Omega_3)] & \frac{1}{2}[(1 - X_3) + (\Omega_2 - \Omega_1)] \\ \frac{1}{2}[(1 - X_1) - (\Omega_3 - \Omega_2)] & \frac{1}{2}[(1 - X_2) - (\Omega_1 - \Omega_3)] & \frac{1}{2}[(1 - X_3) - (\Omega_2 - \Omega_1)] \end{pmatrix}. \quad (26)$$

Although in general the parameters  $\Omega_i$  have the range,  $-1 \leq \Omega_i \leq +1$ , given the current data, it will be seen (Sec. IV and V) that they are all small,  $|\Omega_i| \lesssim O(10^{-1})$ , while vanishing values are not excluded.

FIG. 1: At the  $1\sigma$  level, the measured values for  $\Omega_1^0 - \Omega_2^0$  are bounded by the dashed lines [3] and the dot-dashed lines [4], while the bound on  $\Omega_3^0$  can be represented by the solid lines. It is seen that the two parallelograms allowed by Refs. [3] and [4] do not overlap at the  $1\sigma$  level.



#### IV. NEUTRINO MIXING IN VACUUM

Having settled on the parameter set  $(X_i, \Omega_i)$ , we turn now to the question of their actual numerical values. Since the experimental measurements have been given in terms of the standard parametrization, we need to transcribe the results into the  $(X_i, \Omega_i)$  variables. In so doing, some informations are bound to be lost in translation. Our numerical results are thus only approximate. More precise ones can only be obtained by analyzing directly the experiments in terms of the parameters  $(X_i, \Omega_i)$ .

For the actual numbers we will use the summaries from existing global analyses [3, 4], after making the proper conversion of variables.

First, the  $X_i$ 's are all well-determined. There are slight differences between the two global analyses. Also, the cases for normal and inverted mass spectra are not significantly different. We quote, approximately,  $X_2^0 = 0.32 \pm 0.016$  [3];  $X_2^0 = 0.31 \pm 0.016$  [4], and  $X_3^0 = 0.025 \pm 0.003$  [3];  $X_3^0 = 0.026 \pm 0.003$  [4]. Of course,  $X_1^0 = 1 - X_2^0 - X_3^0$ .

Our knowledge on  $\Omega_i^0$  is far less certain. At the  $1\sigma$  level, we have  $\Omega_1^0 - \Omega_2^0 = 0.14$  to  $0.24$  [3];  $= -0.14$  to  $0.08$  [4]. The discrepancy between these two results, as well as the large percentage errors in each, is a reflection of the poor quality of them.

To complete the list we need one more piece of information on  $\Omega_i^0$ . Despite the lack of another independent measurement, it turns out that the known values of  $X_i^0$  can already set a stringent bound on  $\Omega_3^0$ . To see that we return to Eq. (12) in Sec II,

$$V_{e1}V_{e2}V_{e3}^*V_{\mu3}V_{\tau3} = (y_1y_2 - x_1x_2) + iJ(1 - |V_{e3}|^2). \quad (27)$$

This equation is especially useful if  $|V_{e3}|^2 = \epsilon^2 \ll 1$ . In this case its LHS is significantly bounded since, in general,  $|V_{e1}|^2|V_{e2}|^2 \leq 1/4$  and  $|V_{\mu3}|^2|V_{\tau3}|^2 \leq 1/4$ . (*E.g.*,  $4|V_{e1}|^2|V_{e2}|^2 =$

$(|V_{e1}|^2 + |V_{e2}|^2)^2 - (|V_{e1}|^2 - |V_{e2}|^2)^2 \leq 1)$ . Now,

$$2(y_1 y_2 - x_1 x_2) = -(X_2 \Omega_1 + X_1 \Omega_2). \quad (28)$$

Using vacuum values,

$$X_2^0 \Omega_1^0 + X_1^0 \Omega_2^0 \cong -\Omega_3^0. \quad (29)$$

This follows from  $\sum \Omega_i(1 - X_i) = 0$ , with the approximation  $X_3 \cong 0$ . For  $V_\nu$  in vacuum, actually  $|V_{e1}^0|^2 |V_{e2}^0|^2 \cong 2/9$  and  $|V_{\mu 3}^0|^2 |V_{\tau 3}^0|^2 \cong 1/4$ . Thus, with  $X_3^0 = \epsilon^2$ ,

$$\left(\frac{\Omega_3^0}{2}\right)^2 + (J^0)^2 \cong \epsilon^2/18, \quad (30)$$

and

$$|\Omega_3^0| \leq \sqrt{2}\epsilon/3 \cong 0.07. \quad (31)$$

Also, in the same approximation,

$$\Omega_1^0 + 2\Omega_2^0 + 3\Omega_3^0 \cong 0. \quad (32)$$

The measured values of  $\Omega_1^0 - \Omega_2^0$  can now be combined with the above bound ( $|\Omega_1^0 + 2\Omega_2^0| \leq 0.21$ ) in a plot in the  $\Omega_1^0 - \Omega_2^0$  plane, as shown in Fig. 1. Here, the solid line correspond to the bound in Eq. (31). We emphasize that this bound is robust, with possible deviations of no more than about 10%, largely from the errors in  $|V_{e3}^0|$ . On the other hand, the dashed [3] and dot-dashed [4] lines have large errors, corresponding to the considerable uncertainties in  $\Omega_1^0 - \Omega_2^0$ . Nevertheless, the allowed regions for  $\Omega_1^0$  and  $\Omega_2^0$  (and also  $\Omega_3^0$ ) are essentially confined to the neighborhood of the origin. Despite the significant ambiguities, it seems that a fair assessment is given by  $|\Omega_i^0| \lesssim O(10^{-1})$ .

In summary, given the incomplete results that are available at the present, one can already deduce useful and quantitative information about all of the four physical parameters in  $(X_i^0, \Omega_i^0)$ . Clearly, the next step would be to have a precision measurement on  $\Omega_i^0$ . It is most useful to concentrate on  $\Omega_3^0$ , since this is equivalent to a measurement of  $J^0$ , according to Eq. (30).

Experimentally, the determination of  $\Omega_3^0$  can be quite challenging. First, it is small ( $\lesssim 0.07$ ). Second, its contribution to neutrino oscillation probabilities is not easily disentangled. We recall that the probability for  $\nu^\alpha \rightarrow \nu^\beta$  oscillation is given by

$$P(\nu^\alpha \rightarrow \nu^\beta) = \delta_{\alpha\beta} - 4 \sum_{i>j} Re(\Pi_{ij}^{\alpha\beta}) \sin^2 \Phi_{ij} \pm 8(1 - \delta_{\alpha\beta})J(\sin \Phi_{21} \sin \Phi_{31} \sin \Phi_{32}), \quad (33)$$

where  $\Phi_{ij} = \Delta_{ij}L/4E$ . The amplitudes  $Re(\Pi_{ij}^{\alpha\beta})$  are simple functions of  $W_{\alpha i}$ , or  $X_i$  and  $\Omega_i$ , according to Eq. (11), and are listed in Table I. In this table, it is sufficient to list  $Re(\Pi_{ij}^{\alpha\beta})$  with  $(\alpha, \beta) = (e, \mu)$ . This is because  $\sum_\alpha Re(\Pi_{ij}^{\alpha\beta}) = 0$ , also  $Re(\Pi_{ij}^{\alpha\beta}) = Re(\Pi_{ij}^{\beta\alpha})$ , since  $\Pi_{ij}^{\alpha\beta} = (\Pi_{ij}^{\beta\alpha})^*$ . For vacuum values,  $\Phi_{31}^0 \simeq \Phi_{32}^0$ , so we also list separately the combinations  $Re(\Pi_{31}^{\alpha\beta}) + Re(\Pi_{32}^{\alpha\beta})$ .

In searching for amplitudes that contain  $\Omega_3$ , it is clear that, while  $Re(\Pi_{31}^{\alpha\beta})$  or  $Re(\Pi_{32}^{\alpha\beta})$  does depend on  $\Omega_3$ , once we make the combination  $Re(\Pi_{31}^{\alpha\beta} + \Pi_{32}^{\alpha\beta})$ , very few amplitudes have that property. In fact, the six amplitudes of the form  $Re(\Pi_{21}^{\alpha\beta})$  and  $Re(\Pi_{31}^{\alpha\beta} + \Pi_{32}^{\alpha\beta})$

$Re(\Pi_{21}^{ee})$	$W_{e1}W_{e2}$
$Re(\Pi_{31}^{ee})$	$W_{e1}W_{e3}$
$Re(\Pi_{32}^{ee})$	$W_{e2}W_{e3}$
$Re(\Pi_{31}^{ee} + \Pi_{32}^{ee})$	$W_{e3}(1 - W_{e3})$
$Re(\Pi_{21}^{\mu\mu})$	$W_{\mu1}W_{\mu2}$
$Re(\Pi_{31}^{\mu\mu})$	$W_{\mu1}W_{\mu3}$
$Re(\Pi_{32}^{\mu\mu})$	$W_{\mu2}W_{\mu3}$
$Re(\Pi_{31}^{\mu\mu} + \Pi_{32}^{\mu\mu})$	$W_{\mu3}(1 - W_{\mu3})$
$Re(\Pi_{21}^{\mu e})$	$W_{e1}W_{\mu2} - x_1$
$Re(\Pi_{31}^{\mu e})$	$W_{e1}W_{\mu3} - y_1$
$Re(\Pi_{32}^{\mu e})$	$W_{e2}W_{\mu3} - x_2$
$Re(\Pi_{31}^{\mu e} + \Pi_{32}^{\mu e})$	$-W_{e3}W_{\mu3}$

TABLE I: The amplitudes  $Re(\Pi_{ij}^{\alpha\beta})$  are simple functions of  $W_{\alpha i}$ , or  $X_i$  and  $\Omega_i$ .

fall into three groups. 1)  $Re(\Pi_{21}^{ee})$  and  $Re(\Pi_{31}^{ee} + \Pi_{32}^{ee})$ : They do not contain  $\Omega_i$ , and have been used to determine  $X_i^0$  successfully. 2)  $Re(\Pi_{31}^{\mu\mu} + \Pi_{32}^{\mu\mu})$  and  $Re(\Pi_{31}^{\mu e} + \Pi_{32}^{\mu e})$ . Here,  $W_{\mu3}(1 - W_{\mu3}) \simeq \frac{1}{4}[1 - (\Omega_2 - \Omega_1)^2]$ , and  $-W_{e3}W_{\mu3} \simeq -X_3[1 + (\Omega_2 - \Omega_1)]/2$ , for  $X_3 \ll 1$ . Thus, for vacuum values, they can only be used to determine  $(\Omega_2^0 - \Omega_1^0)$ . 3) The amplitude  $Re(\Pi_{21}^{\mu\mu})$  and  $Re(\Pi_{21}^{\mu e})$  do depend on  $\Omega_3$ . Substituting in the approximate vacuum values,  $X_1^0 \simeq 2/3$ ,  $X_2^0 \simeq 1/3$ ,  $X_3^0 \approx 0$ , and dropping quadratic terms in  $\Omega_i$ , we find  $Re(\Pi_{21}^{\mu\mu})^0 \simeq \frac{1}{18} - \frac{1}{6}(2\Omega_2^0 + \Omega_3^0)$ ,  $Re(\Pi_{21}^{\mu e})^0 \simeq -\frac{1}{9} + \frac{1}{6}(2\Omega_2^0 + \Omega_3^0)$ .

Thus, to gain access to  $\Omega_3^0$  (actually  $\Omega_3^0 + 2\Omega_2^0$ ), one has to isolate the amplitudes  $Re(\Pi_{21}^{\mu\mu})^0$  and  $Re(\Pi_{21}^{\mu e})^0$ , which is by no means easy. We can only hope that the technical difficulties involved can be overcome in the near future.

## V. NEUTRINO MIXING IN MATTER

When neutrinos propagate in matter, their interactions induce a term in the effective Hamiltonian, given by  $(H)_{ee} = A = 2\sqrt{2}G_F n_e E$  [14]. The mass eigenvalues and the mixing matrix are now functions of  $A$ . It was shown [15] that they satisfy a set of differential equations listed in Table II, together with

$$\frac{dD_i}{dA} = X_i. \quad (34)$$

These equations are derived from

$$(V + dV)^\dagger (H + dH) (V + dV) = D + dD, \quad (35)$$

which is just the flavor-basis version of the familiar perturbation theory in quantum mechanics,

$$(1 + dV)^\dagger (H + dH) (1 + dV) = D + dD, \quad (36)$$

written in the mass eigenstate basis. Thus, the quantum mechanical result  $dD_i = \langle i | dH | i \rangle$  becomes Eq. (34),  $dD_i = |V_{ei}|^2 dA$ , when  $dH$  has only an  $(ee)$  element,  $\langle e | dH | e \rangle = dA$ .



	$1/\Delta_{12}$	$1/\Delta_{23}$	$1/\Delta_{31}$
$\frac{1}{2} \frac{d}{dA} \ln X_1$	$X_2$		$-X_3$
$\frac{1}{2} \frac{d}{dA} \ln X_2$	$-X_1$	$X_3$	
$\frac{1}{2} \frac{d}{dA} \ln X_3$		$-X_2$	$X_1$
$\frac{d\Omega_1}{dA}$	$\Omega_1 X_2 - \Omega_2 X_1$	$-\Omega_1 X_2 - \Omega_2 X_1 + \Omega_1 X_3 + \Omega_3 X_1$	$-\Omega_1 X_3 + \Omega_3 X_1$
$\frac{d\Omega_2}{dA}$	$\Omega_1 X_2 - \Omega_2 X_1$	$\Omega_2 X_3 - \Omega_3 X_2$	$\Omega_1 X_2 + \Omega_2 X_1 - \Omega_2 X_3 - \Omega_3 X_2$
$\frac{d\Omega_3}{dA}$	$-\Omega_1 X_3 - \Omega_3 X_1 + \Omega_2 X_3 + \Omega_3 X_2$	$\Omega_2 X_3 - \Omega_3 X_2$	$-\Omega_1 X_3 + \Omega_3 X_1$

TABLE II: The differential equations for  $X_i$  and  $\Omega_i$  in matter, expressed as the sums of terms proportional to  $1/\Delta_{ij}$ .

Similarly, the equations for  $X_i$  and  $\Omega_i$  are just rephasing invariant combinations constructed out of the well-known formula  $dV_{ij} = \langle i|dH|j\rangle/(D_j - D_i)$ , after its conversion into the flavor basis.

The above arguments should help to illuminate the nature of these differential equations and to put on firm grounds the use of them in solving the mixing problem. It is noteworthy that the equations for  $D_i$  and  $X_i$  are independent of  $\Omega_i$ . These equations are even under  $P_{\mu\tau}$  so that, barring the possible appearance of higher order terms, the  $\Omega$ 's are absent. Similarly, the differential equations for  $\Omega_i$  are odd under  $P_{\mu\tau}$ , so that they are all linear in  $\Omega_i$ . Previously [15], we studied the  $A$ -dependence of  $X_i$  and  $D_i$ , assuming  $\Omega_i = 0$ . We now see that even with  $\Omega_i \neq 0$ , the conclusions remain valid. We only need to add  $\Omega_i$  to the list and find out how they behave.

Let us first summarize the results for  $X_i$  and  $\Omega_i$ . Because the mass differences  $\Delta_{21}^0$  and  $\Delta_{32}^0$  are widely separated, it is known (see *e.g.*, Ref. [17]) that the three-flavor problem can be well approximated by two, two-flavor, level crossing problems, occurring at  $A = A_l$ , when  $\Delta_{21} = \min$ , and at  $A = A_h$ , for  $\Delta_{32} = \min$ . In our present formulation this is just the pole dominance approximation. Near  $A \sim A_l$ , the differential equations for  $(D_1, D_2, X_1, X_2)$  are reduced to the pole term  $\propto 1/D_{21}$ , plus Eq. (34). Similarly, for  $A \sim A_h$ , variations of  $(D_2, D_3, X_2, X_3)$  are governed by Eq. (34) and the pole term  $\propto 1/D_{32}$ . Consequently, the function  $D_i(A)$  takes turn to rise linearly, while  $X_i$  behaves as step-functions. We list these results by dividing  $A$  into three regions,

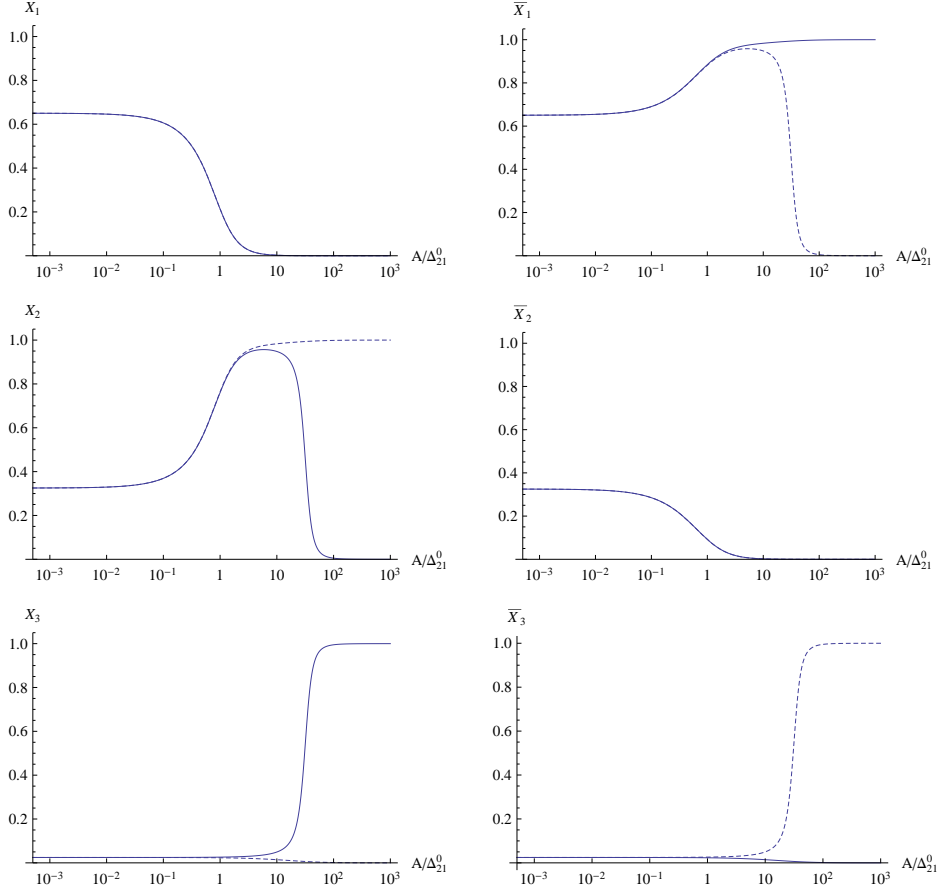
I)  $A \lesssim A_l$ :  $D_1 \propto X_1^0 A$ ,  $D_2 \propto X_2^0 A$ ,  $D_3 \cong \text{constant}$ ,  $X_i \cong X_i^0$ ;

II) intermediate  $A_i$  region,  $A_l \lesssim A \lesssim A_h$ :  $(D_1, D_3) \cong \text{constant}$ ,  $D_2 \propto A$ ,  $X_1 \rightarrow 0$ ,  $X_2 \rightarrow 1$ ,  $X_3 \cong X_3^0$ ;

III) dense medium  $A_d$ ,  $A \gtrsim A_h$ :  $(D_1, D_2) \cong \text{constant}$ ,  $D_3 \propto A$ ,  $(X_1, X_2) \rightarrow 0$ ,  $X_3 \rightarrow 1$ . Detailed graphs for these variables will be given in Sec. VI.

Having obtained the functions  $D_i(A)$  and  $X_i(A)$ , we can now use them to evaluate  $\Omega_i(A)$ . While one can integrate the differential equations for  $\Omega_i$  (Table II) numerically, which will be presented in Sec. VI, much of the behavior of  $\Omega_i(A)$  can already be inferred from the constraints (Eq. (21)) and the nature of the differential equations they satisfy. As with  $X_i(A)$  and  $D_i(A)$ , we will now invoke the pole dominance approximation, so that  $\Omega_i(A)$  undergo rapid variations only near the resonances  $A \sim A_l$  and  $A \sim A_h$ . Outside of these,  $\Omega_i(A)$  are essentially flat. Their values can be summarized as follows.

FIG. 2: The parameters  $X_i$  (left column) and  $\bar{X}_i$  (right column) as functions of  $A/\Delta_{21}^0$  for both the normal (solid) and the inverted (dashed) mass spectra. The initial values in vacuum are well-measured, with  $X_1^0 = \bar{X}_1^0 \simeq (2/3)(1 - X_3^0)$ ,  $X_2^0 = \bar{X}_2^0 \simeq (1/3)(1 - X_3^0)$ , where  $X_3^0 = \bar{X}_3^0 = |V_{e3}^0|^2$ .



I) In the intermediate  $A$  region,  $A_l \lesssim A \lesssim A_h$ :  $\Omega_1 \rightarrow 0$ ,  $\Omega_2 \rightarrow \Omega_2^0 - \Omega_1^0$ ,  $\Omega_3 \rightarrow 0$ . Here,  $X_1 \rightarrow 0$ ,  $X_2 \rightarrow 1 - X_3^0 \cong 1$ ,  $X_3 \rightarrow X_3^0$ . Also, a more precise  $X_1(A)$  can be obtained by using  $X_1^0 X_2^0 (\Delta_{21}^0)^2 = X_1 X_2 (\Delta_{21})^2$  (Eq. (4.12) of Ref. [12]). With  $X_2 \rightarrow 1$ ,  $(\Delta_{21})^2 \cong A^2$ , and  $X_1^0 X_2^0 \cong 2/9$ , we have  $X_1(A) \cong (2/9)(\Delta_{21}^0/A)^2$ , for  $A_l \lesssim A \lesssim A_h$ .  $X_1(A)$  is thus already very small for  $A \gtrsim 5\Delta_{21}^0$ . Now we turn to the identity Eq. (13), for  $\alpha = e$ ,  $l = 1$ ,

$$V_{\mu 1} V_{\tau 1} V_{e 1}^* V_{e 2} V_{e 3} = (-x_2 x_3 + y_2 y_3) + iJ(1 - |V_{e 1}|^2). \quad (37)$$

With  $|V_{e 1}| = \epsilon' \ll 1$ ,  $|V_{\mu 1} V_{\tau 1}| \leq 1/2$ ,  $|V_{e 3}| = \epsilon \ll 1$ , and  $\Omega_1 \cong -(\Omega_2 X_3 + \Omega_3 X_2) = -2(x_2 x_3 - y_2 y_3)$ , we find the bound

$$|\Omega_1| \leq \epsilon \epsilon', \quad (38)$$

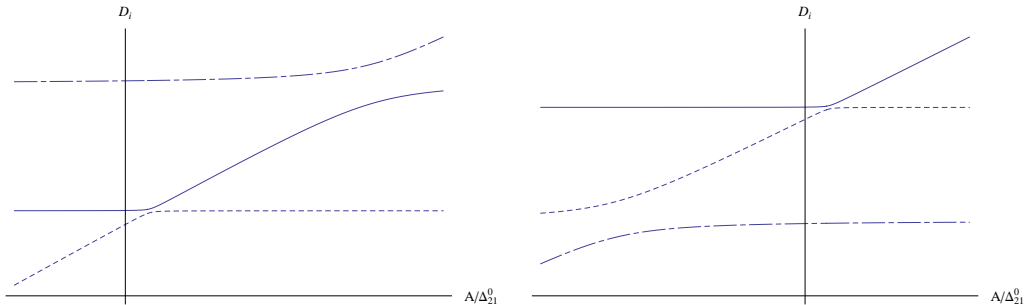
for  $A_l \lesssim A \lesssim A_h$ . At the same time, the constraint  $\sum \Omega_i (1 - X_i) = 0$ , after putting in the values of  $X_i$ , becomes

$$\Omega_1 + \Omega_3 \cong 0. \quad (39)$$

Finally, referring to Table II, we have

$$\frac{d}{dA}(\Omega_2 - \Omega_1) = 0, \quad (40)$$

FIG. 3: The qualitative plots for  $D_1$  (dashed),  $D_2$  (solid), and  $D_3$  (dot-dashed) under normal (left) and inverted (right) hierarchies. Note that in each plot, the curves in the positive region of  $A$  represent  $D_i$  for the  $\nu$ -sector, while that in the negative region of  $A$  represent  $D_i$  for the  $\bar{\nu}$ -sector.



at the  $A_l$  pole. Thus,

$$\Omega_2^0 - \Omega_1^0 = \Omega_2 - \Omega_1 \rightarrow \Omega_2(A) \quad (41)$$

for  $A_l \lesssim A \lesssim A_h$ .

II) For dense medium,  $A \gtrsim A_h$ :  $\Omega_1 \rightarrow 0$ ,  $\Omega_2 \rightarrow 0$ ,  $\Omega_3 \rightarrow -\Omega_2^0 + \Omega_1^0$ . In this region,  $X_1 \rightarrow 0$ ,  $X_2 \rightarrow 0$ ,  $X_3 \rightarrow 1$ . Following steps as above, we see first that  $\Omega_2 \rightarrow 0$ . The constraint equation then gives  $\Omega_1 + \Omega_2 = 0$ , and, using the property of the pole at  $A_h$ ,  $d(\Omega_3 - \Omega_2)/dA = 0$ , we find the results listed. Note that the initial conditions for the differential equation are  $\Omega_3(A_i) = 0$ ,  $\Omega_2(A_i) = \Omega_2^0 - \Omega_1^0$ .

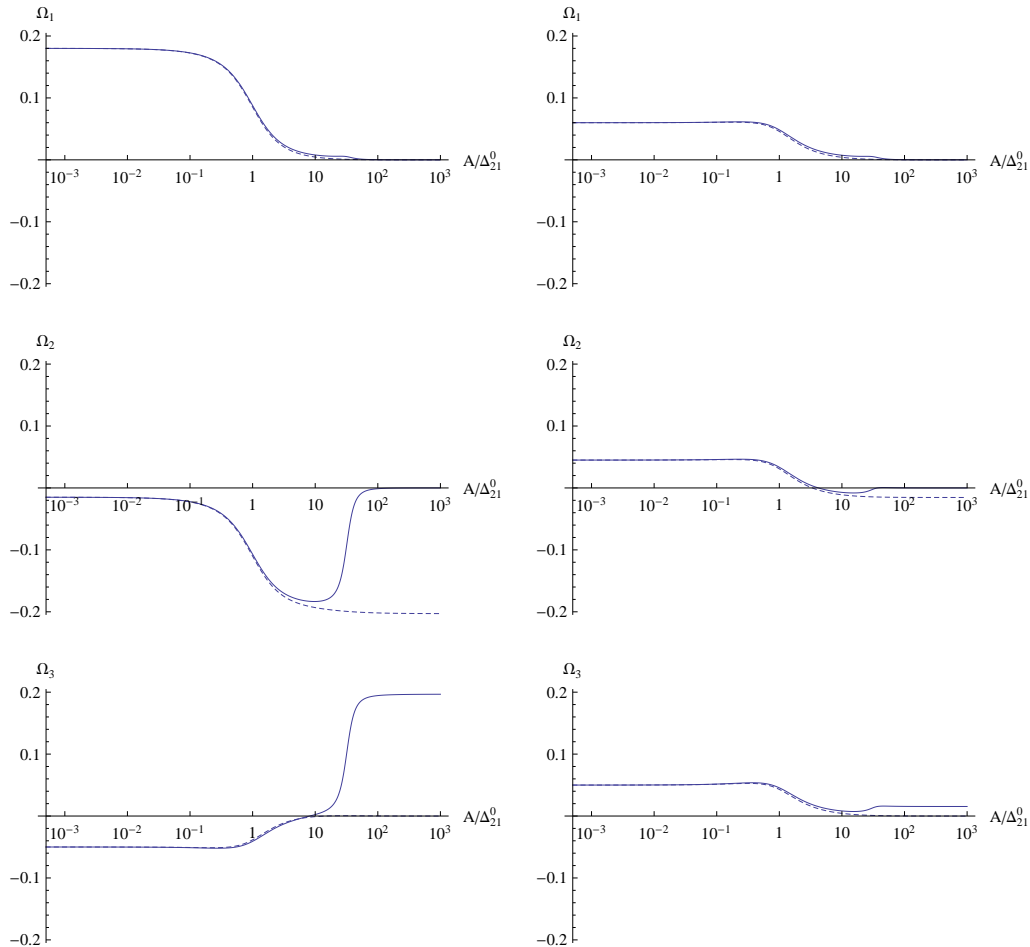
Our results show that  $\Omega_i(A)$  behave rather simply as functions of  $A$ . The transition regions near  $A_l$  and  $A_h$ , however, are not covered. For these we need to solve the differential equations numerically, which will be given in Sec. VI. After these transition regions, the resonances act to “quench” many of the parameters. Thus, as  $A$  increases, much of the information in the original set  $(X_i^0, \Omega_i^0)$  will disappear, and  $W_\nu$  contains fewer and fewer free parameters. Physically, this is a consequence of the decoupling of the  $|e\rangle$  state, whose mass rises roughly as a linear function of  $A$ . Starting as a mixture of  $|1\rangle$  and  $|2\rangle$ , it evolves into an almost pure  $|2\rangle$  state, and eventually becomes just a  $|3\rangle$  state. For  $A \gg m_3^2$ , the system is made up of  $|e\rangle$  ( $|3\rangle$ ) plus a completely decoupled two-flavor system, consisting of  $|\mu\rangle$  and  $|\tau\rangle$ , or  $|1\rangle$  and  $|2\rangle$ . The vestige of the original  $\mu - \tau$  mixing,  $(\Omega_2^0 - \Omega_1^0)$ , however, remains undisturbed by the change in the  $e$ -channel, coming from  $\Delta H_{ee}$ .

So far we have tacitly assumed the “normal” ordering of the neutrino masses. For the case of “inverted” ordering, the resonance at  $A_h$  is absent, but the rest of our analyses remain valid.

## VI. NUMERICAL SOLUTIONS

We summarize our analyses of the parameters here with their numerical solutions. As indicated earlier, the quantities  $X_i^0$  and  $\Delta_{ij}^0 = D_i - D_j$  are all well measured at  $A = 0$ , with errors  $\sim 10\%$ . We show both  $X_i$  (for  $\nu$ ) and  $\bar{X}_i$  (for  $\bar{\nu}$ ) as functions of  $A/\Delta_{21}^0$  in Fig. 2 with the initial values:  $X_1^0 = \bar{X}_1^0 \simeq (2/3)(1 - X_3^0)$  and  $X_2^0 = \bar{X}_2^0 \simeq (1/3)(1 - X_3^0)$ , where  $X_3^0 = \bar{X}_3^0 = |V_{e3}^0|^2$  is taken from both Refs. [3] and [4]. It is seen that the paths for  $\nu$  and  $\bar{\nu}$  begin to evolve apart when  $A \gtrsim A_l$ . In addition,  $X_1$  and  $\bar{X}_2$  are insensitive to the mass hierarchy, while each of  $X_2$ ,  $X_3$ ,  $\bar{X}_1$ , and  $\bar{X}_3$  evolves diversely under different

FIG. 4: The numerical solutions of  $\Omega_i$  for the  $\nu$ -sector under both the normal hierarchy (solid) and the inverted hierarchy (dashed). Two different sets of initial values are adopted:  $(\Omega_1^0, \Omega_2^0, \Omega_3^0) = (0.18, -0.015, -0.05)$  [3] (left column) and  $(\Omega_1^0, \Omega_2^0, \Omega_3^0) = (0.06, 0.045, 0.05)$  [4] (right column).



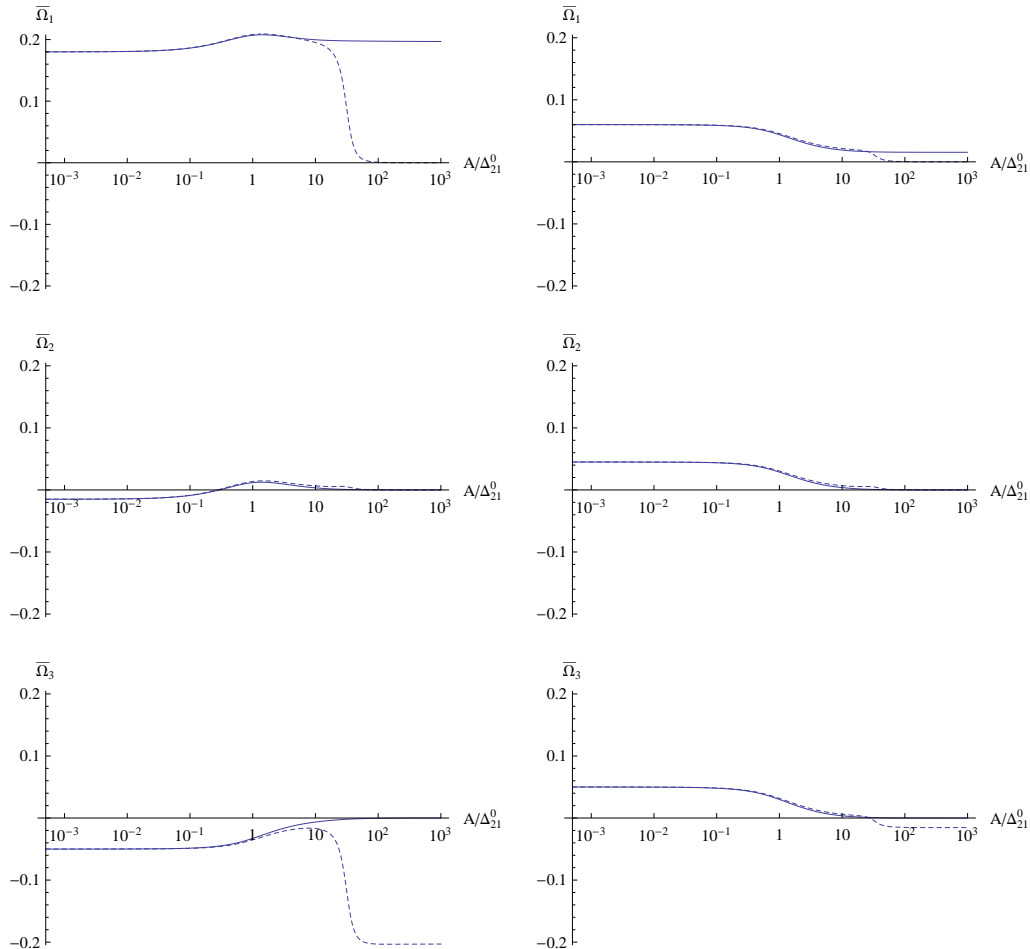
mass hierarchies when  $A > A_l$ , where the higher resonance begins to affect. Note that with the exchange: normal  $\leftrightarrow$  inverted, the “trends” of the following curves evolve similarly:  $X_1 \sim \bar{X}_2$ ,  $X_2 \sim \bar{X}_1$ , and  $X_3 \sim \bar{X}_3$ . The evolution details of  $X_i$  and  $\bar{X}_i$  can be readily inferred from how  $D_i$  varies, as indicated by Eq. (34). As an illustration, we provide the well-known qualitative plots of  $D_i$  in Fig. 3.

On the other hand,  $\Omega_i^0$  are only roughly known from global fits, with typical errors of  $30 \sim 100\%$ . The evolution equations for  $\Omega_i$  in Table II can be expressed in a compact form,

$$\begin{aligned} \frac{d\Omega_i}{dA} = & \sum_{j>k} \frac{1}{\Delta_{jk}} [\delta_{ij}(\Omega_i X_k - \Omega_k X_i) - \delta_{ik}(\Omega_i X_j - \Omega_j X_i)] \\ & + \sum_{j>k, i \neq j \neq k} \frac{1}{\Delta_{jk}} [-(\Omega_i X_j + \Omega_j X_i) + (\Omega_i X_k + \Omega_k X_i)]. \end{aligned} \quad (42)$$

The numerical solutions of  $\Omega_i$  for both mass spectra are shown in Fig. 4. It is seen that the evolution of  $\Omega_i$  is sensitive to the choice of initial values, which are not quite settled experimentally. The general features, however, can be fairly understood from the constraint, Eq. (21), and the nature of the evolution equations, as discussed in Sec. V. Note that the

FIG. 5: The numerical solutions of  $\bar{\Omega}_i$  for the  $\bar{\nu}$ -sector under both the normal hierarchy (solid) and the inverted hierarchy (dashed). We adopt two different sets of initial values:  $(\Omega_1^0, \Omega_2^0, \Omega_3^0) = (0.18, -0.015, -0.05)$  [3] (left column) and  $(\Omega_1^0, \Omega_2^0, \Omega_3^0) = (0.06, 0.045, 0.05)$  [4] (right column).



curves for the inverted mass ordering follow more closely the trend we discussed in Sec. V since they are not distorted by the higher resonance.

For the  $\bar{\nu}$ -sector, the evolution of  $\bar{\Omega}_i$  in matter is shown in Fig. 5. The analyses in Sec. IV remain valid to the understanding of their general features. Note that  $\Omega_i$  ( $\bar{\Omega}_i$ ) share similar qualitative properties as  $X_i$  ( $\bar{X}_i$ ), *e.g.*,  $\Omega_1$  and  $\bar{\Omega}_2$  are insensitive to the mass hierarchy even when the neutrinos propagate in matter, while the matter effect breaks the hierarchy degeneracy for each of the parameters,  $\Omega_2$ ,  $\Omega_3$ ,  $\bar{\Omega}_1$ , and  $\bar{\Omega}_3$ , when  $A > A_l$ .

As one scans through the plots, it is noteworthy that all of the parameters undergo rapid changes near the resonance positions, but are otherwise more or less flat. This lends support to the use of the pole approximation in Sec. V. The values before and after the transition regions also agree with the estimates given in Sec. V. For instance, consider Fig. 4. Here,  $\Omega_1$  drops from  $\Omega_1^0 = 0.18$  to almost zero, when  $A/\Delta_{21}^0$  varies from about 0.5 to 3. At the same time,  $\Omega_3$  changes from  $-0.05$  to  $\sim 0$ , while  $\Omega_2$  goes from  $-0.01$  to  $\sim -0.18$ , not far from  $\Omega_2^0 - \Omega_1^0 \approx -0.19$ . From  $A/\Delta_{21}^0 \sim 3$  to  $\sim 25$ ,  $\Omega_i$  stays nearly constant. The other plots can be similarly analyzed. To summarize, unless very high accuracy is demanded, the approximation presented in Sec. V should be sufficient for most purposes.

## VII. CONCLUSION

The physics of neutrino oscillation is governed by a mixing matrix  $V_\nu$  which is unitary, unimodular, and rephasing invariant. As such  $V_\nu$  (or  $W_\nu$ ) satisfies a number of self-consistency conditions (such as Eq. (13)) which can help to characterize the matrix. To exploit these properties, we propose to use the parameters  $X_i$  ( $= W_{ei}$ ) and  $\Omega_i$  ( $= \varepsilon_{ijk} W_{\mu j} W_{\tau k}$ ), which satisfy two constraints, Eq. (18) and Eq. (21). Physically, the set  $\Omega_i$  offers a measure of the  $\mu - \tau$  asymmetry. These parameters are directly measurable, since the neutrino oscillation probabilities  $P(\nu^\alpha \rightarrow \nu^\beta)$  are simple functions of them. This parametrization is summarized in Eq. (26).

Experimentally, the vacuum values of  $X_i$  ( $X_i^0$ ) are well-determined. But for  $\Omega_i$  there is only one measurement on  $(\Omega_2^0 - \Omega_1^0)$ , which turns out to be small ( $O(10^{-1})$ ), with large uncertainties. However, using Eq. (27), one can establish the bound  $\Omega_3^0 \lesssim 0.07$ , whose validity depends on the approximation  $X_3^0 \ll 1$ . There is also a sum rule relating  $\Omega_3^0$  to  $J^0$ , Eq. (30). It is thus urgent to have a precision measurement on  $\Omega_3^0$ , although the task can be very challenging.

Turning to neutrino propagation in matter, we find that the parameters have simple dependences on  $A$ , the induced mass. To a good approximation, there are two resonance regions ( $A \sim A_l$  and  $A \sim A_h$ ) where they change rapidly. Outside of these there are three regions of  $A$  in which all parameters take on values that are nearly constant. These are given in detail in Sec. V. Starting from  $(X_i^0, \Omega_i^0)$  for vacuum ( $A = 0$ ), the list of free parameters gets shorter as  $A$  increases. For  $A_l \lesssim A \lesssim A_h$ , there are only two:  $\Omega_2(A_i) \cong \Omega_2^0 - \Omega_1^0$ ,  $X_3(A_i) \cong X_3^0$ . For  $A \gtrsim A_h$ , it is down to one:  $\Omega_3(A_d) \cong -(\Omega_2^0 - \Omega_1^0)$ . Physically, this behavior is a consequence of decoupling, and can be tested in LBL experiments. So far, the analysis is done under the assumption of normal hierarchy. For the case of inverted hierarchy, similar results are obtained with the omission of the higher resonance.

In conclusion, given the incomplete knowledge that is now available, it is seen that, with the help of consistency conditions and the approximations  $X_3^0 \ll 1$  and  $\Delta_{21}^0 \ll \Delta_{31}^0$ , much can already be learned quantitatively about  $W_\nu$ , both in vacuum and in matter. It is hoped that our analysis will be helpful toward establishing a comprehensive specification of the neutrino mixing matrix.

### Acknowledgments

SHC is supported by the National Science Council of Taiwan, Grant No. NSC 100-2112-M-182-002-MY3.

- 
- [1] Daya Bay Collaboration, Phys. Rev. Lett. **108**, 171803 (2012).
  - [2] RENO Collaboration, Phys. Rev. Lett. **108**, 191802 (2012).
  - [3] G. L. Fogli *et al.*, hep-ph/1205.5254.
  - [4] D. V. Forero *et al.*, hep-ph/1205.4018.
  - [5] C. H. Albright *et al.*, physics/0411123 (2004).
  - [6] ISS Physics Working Group (A. Bandyopadhyay *et al.*), Rept. Prog. Phys. **72**, 106201 (2009); hep-ph/0710.4947.

- [7] P. F. Harrison and W. G. Scott, Phys. Lett. B **547**, 219 (2002).
- [8] C. S. Lam, Phys. Lett. B **507**, 214 (2001).
- [9] T. K. Kuo and T.-H. Lee, Phys. Rev. D **71**, 093011 (2005).
- [10] S. H. Chiu, T. K. Kuo, T.-H. Lee, and C. Xiong, Phys. Rev. D **79**, 013012 (2009).
- [11] S. H. Chiu, T. K. Kuo, and Lu-Xin Liu, Phys. Lett. B **687**, 184 (2010).
- [12] S. H. Chiu and T. K. Kuo, JHEP **11**, 080 (2010), Erratum-*ibid.* **01**, 147 (2011).
- [13] J. Beringer et al. (Particle Data Group), Phys. Rev. D **86**, 010001 (2012).
- [14] L. Wolfenstein, Phys. Rev. D **17**, 2369 (1978); S. P. Mikheyev and A. Yu. Smirnov, Yad. Fiz. **42**, 1441 (1985) [Sov. J. Nucl. Phys. **42**, 913 (1985)].
- [15] S. H. Chiu and T. K. Kuo, Phys. Rev. D **84**, 013001 (2011).
- [16] C. Jarlskog, Phys. Rev. Lett. **55**, 1039 (1985).
- [17] T. K. Kuo and J. Pantaleone, Rev. Mod. Phys. **61**, 937 (1989).